ACS Photonics

Article

pubs.acs.org/journal/apchd5

Optofluidic Lasers with Aqueous Quantum Dots

Alper Kiraz,*[,†,‡] Qiushu Chen,[‡] and Xudong Fan*[,‡]

[†]Department of Physics, Koç University, Rumelifeneri Yolu, Sariyer, 34450 Istanbul, Turkey

[‡]Department of Biomedical Engineering, University of Michigan, Ann Arbor, Michigan 48109, United States

Supporting Information

ABSTRACT: We achieved two types of laser emissions from aqueous quantum dots (QDs) using the same high-Q-factor optofluidic ring resonator (OFRR) platform. In the first type, 2 μM QDs were in bulk buffer solution that filled the entire OFRR cavity volume. The lasing threshold was 0.1 μJ/mm^2, over 3 orders of magnitude lower than the state-of-the-art. In the second type of laser, the QDs were immobilized as a single layer on the interface between the OFRR inner wall and buffer solution with a surface density as low as 3×10^9–10^{10} cm^{-2}. The lasing threshold of 60 μJ/mm^2 was achieved. In both bulk solution and single-layer lasing cases, the laser emission persisted even under 5–10 min of uninterrupted pulsed optical excitation that was well above the corresponding lasing threshold, indicative of high photostability of the QD laser. This was in sharp contrast to organic-dye-based lasers, which underwent quick photobleaching during the laser operation under similar pumping conditions. Theoretical analysis is also carried out to elucidate the advantages of QD-based optofluidic lasers over those based on dyes. Our work opens the door to a plethora of applications where optofluidic QD lasers can replace dye-based optofluidic lasers in biosensing and on-chip miniaturized laser development.

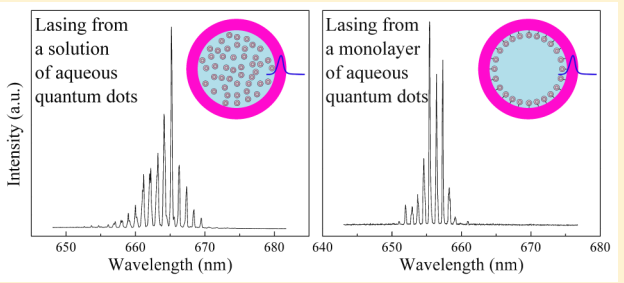

KEYWORDS: *quantum dot, optofluidic ring resonator, laser, optofluidic laser*

Optofluidic lasers have recently emerged as exquisite new tools for biosensing applications.[1−3] Optofluidic laser biosensors contain the fluorescently labeled analytes as an integral part of the laser gain medium. Benefiting from the high sensitivity of stimulated emission to small perturbations in the laser cavity and gain medium, optofluidic laser biosensors have been applied to DNAs,[4−7] proteins,[8] cells,[9,10] and tissues[11,12] to reveal subnanometer conformational changes in biomolecules,[4] distinguish small thermal dynamic differences between two biomolecules,[5,6] analyze structures and morphologies of cells and tissues,[10−12] and detect biomarkers at extremely low concentrations (~1 fg/mL),[13] all of which cannot easily be achieved with standard fluorescence techniques based on spontaneous light emission. Optofluidic lasers with the gain medium both in bulk solution[4−6,8,9] and on solid/liquid interfaces[14] have been realized, which is analogous to the traditional fluorescence detection that can be carried out in both bulk solution and on solid/liquid interfaces.

To date, organic dyes have been the most commonly used gain medium for optofluidic lasers. However, organic dyes suffer severely from photobleaching, which makes it very challenging to perform repetitive measurements with long exposure time. The photobleaching issue is exacerbated when the dyes are part of the laser as gain medium and involved in laser emission, where the intracavity light intensity can be even higher. In addition, organic dyes are sensitive to solvent conditions (such as pH, polarity, and ionic strength), making it less attractive when used in different biological systems. In contrast, semiconductor quantum dots (QDs) come together with unique advantages over organic dyes. Core/shell structured QDs can be engineered with optimized passivation layers to achieve monodisperse sizes while possessing high resistance to photobleaching and high quantum yields in the presence of water and other harsh solvents (high acidity, basicity, and salt concentration, *etc.*).[15−18] In addition, QDs have high absorption cross sections,[19−21] which is critical for lasing with low pump intensities. Furthermore, QDs have broad absorption bands and their emission wavelength can be tuned by simply changing their size or composition; different colors of fluorescence can be obtained using the same excitation source. Therefore, QDs have increasingly been used as alternatives to organic dyes for biosensing, imaging, and ion detection applications.[22−24]

Since their invention, QDs have been explored as laser gain medium.[25−31] In those lasers, QDs either form a relatively thick solid film[25] or are embedded in a solid matrix (such as silica[26] and polymer[32]). Only a few demonstrations have employed QDs in a solution as laser gain medium.[33−35] The first solution-based QD laser was reported in 2002 using hexane as the solvent.[33] This work was followed by a very recent work that utilized QDs in toluene as the laser gain medium.[35] Lasing threshold fluences on the order of hundreds of μJ/mm^2 were achieved in these demonstrations. For bioanalysis applications lasing from aqueous QDs with low lasing thresholds is of

Received: January 8, 2015
Published: May 13, 2015

DOI: 10.1021/acsphotonics.5b00211
ACS Photonics 2015, 2, 707−713

critical importance. Unfortunately, to the best of our knowledge, only one related work was reported to date in which lasing was observed from QDs dissolved in glycerol/water microdroplet resonators trapped by an electrodynamic trap.[34] However, the droplet-based laser cavity suffers from sample evaporation, cavity deformation, and lack of microfluidics for sample delivery. Each droplet needs to be prepared separately with poor size and shape control. Therefore, it is difficult to use droplets as practical devices for repetitive and consistent measurements over a relatively long time. In addition, due to the relatively low Q-factor, a high lasing threshold over 400 μJ/mm^2 was needed.

In this paper we achieved low-threshold lasing emission from aqueous QDs when they were in bulk aqueous solution or immobilized as a single layer on the interface between a solid substrate and aqueous solution. Due to the excellent Q-factor of the optical cavity and the high fluorescence quality of the QDs, a lasing threshold fluence of 0.1 μJ/mm^2 was obtained for QDs in bulk solution with a concentration as low as 2 μM, 3 orders of magnitude lower than the state-of-the-art with a similar QD concentration. For QDs immobilized as a single layer with a surface density as low as 3×10^9–10^{10} cm^{-2}, the lasing threshold was 60 μJ/mm^2. In both cases, the QD lasing persisted even under uninterrupted pulsed pumping with 3.5–10 times the lasing threshold fluence for 5–10 min, showing significantly higher resistance to photobleaching than organic dyes, which started to photobleach almost instantaneously upon laser operation under similar pumping conditions. Our work opens the door to a plethora of studies where QDs are used as optofluidic laser gain medium for the development of new types of lasers and for bioanalysis in bulk solutions or at solid/liquid interfaces.

The laser cavity used in our work was an optofluidic ring resonator (OFRR) based on a thin-walled fused silica capillary. The fabrication and characteristics of the OFRR have been well studied in the past few years.[36−39] Briefly, an OFRR with an inner diameter of 70–90 μm and a wall thickness of 1–2 μm was obtained by rapidly stretching a fused silica preform under CO_2 laser illumination.[36,37] The circular cross section of the capillary forms the ring resonator that supports the high-Q (>10^7) whispering gallery modes (WGMs).[38−40] The OFRR is a very versatile cavity that can accommodate liquids with various refractive indices.[39,41] When the gain medium is in liquid having a refractive index lower than that of glass, the WGM is mainly confined within the capillary wall, but has an evanescent field present inside the capillary to provide optical feedback for the gain medium to lase (Figure 1A). On the other hand, when the liquid has a higher refractive index, the WGM exists mainly in the liquid, which also provides optical feedback for lasing. Furthermore, the WGM can interact with a single layer of gain molecules at the solid/liquid interface (Figure 1B).[14] For the present work, in which QD lasing occurs in an aqueous environment (water refractive index ~1.33 at visible wavelengths), we utilized the OFRR's first and third properties described in Figure 1A and B.

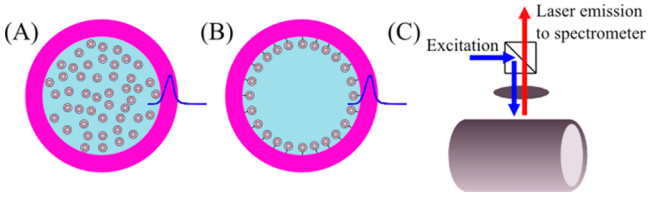

Figure 1. Illustrations of aqueous QDs (A) in solution inside an OFRR and (B) immobilized as a single layer on the inner surface of an OFRR. Qualitative sketches of radial dependence of WGM intensity are also shown in (A) and (B). (C) Illustration of the experimental setup using confocal geometry.

A commercially available QD solution in aqueous buffer (Invitrogen Qdot 655; CdSe/ZnS quantum dots; 2 μM in borate buffer; 8 × 15 nm average QD dimensions[42−44]) was used in the experiments. A representative TEM image of the QDs used in this study is shown in Figure S1 in the Supporting Information. Amine-to-amine cross-linking was used for surface immobilization of the Qdot 655 QDs on the inner surface of the OFRRs. Details of this procedure are described in the Supporting Information. Optical experiments were performed using a confocal setup to excite OFRRs with a pulsed optical parametric oscillator (OPO) (repetition rate: 20 Hz, pulse width: 5 ns) (Figure 1C). An excitation wavelength of 433 nm was used in all the QD experiments. A 25 mm focal distance plano-convex lens was used for focusing the excitation beam at a 0.65 mm spot on the OFRRs (spot size measurement is detailed in the Supporting Information) and collecting the OFRR laser emission. A spectrometer (Horiba 550) and a CCD camera were used for spectral detection of the OFRR laser emission signals.

The inset of Figure 2 shows the emission spectra recorded at various pump intensities from an OFRR filled with a 2 μM QD solution in borate buffer. These measurements and all other measurements reported in this paper were performed in the absence of liquid flow, when the gain medium was kept still inside the OFRR. At a low pump intensity, only spontaneous emission is observed. With increased pump intensity, multiple lasing peaks emerge at the red side of the QD emission band. Multimode lasing is intrinsically observed with ring resonators unless additional mechanisms such as the Vernier effect are employed to ensure single-mode operation.[45] An analysis of the power-dependent spectral intensity for the lasing region between 660 and 665 nm plotted in Figure 2 reveals a lasing

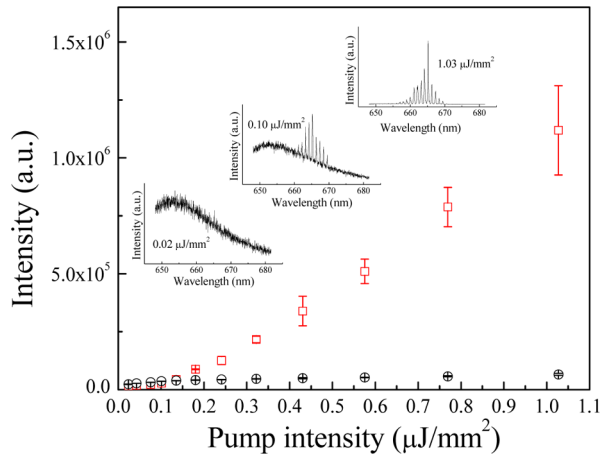

Figure 2. Spectrally integrated intensity as a function of pump intensity for laser emission (squares) and fluorescence (circles) for 2 μM aqueous QDs in borate buffer solution. Spectral integration takes place in the range 660–665 nm for lasing and 650–655 nm for fluorescence. The lasing threshold is 0.1 μJ/mm^2 per pulse. Insets show examples of emission spectra below and above the respective lasing threshold. Error bars are obtained with three measurements.

DOI: 10.1021/acsphotonics.5b00211
ACS Photonics 2015, 2, 707−713

threshold fluence of 0.1 μJ/mm^2. In contrast, the nonlasing part (650−655 nm) of the QD emission spectrum increases sublinearly, and saturation occurs at increased pump intensities. In Figure 2, a red shift of almost 10 nm is observed between the lasing intensity maximum and the spontaneous emission peak. This is attributed to self-absorption, consistent with the previous experiments with dye lasers[39,46] or semiconductor quantum well lasers.[47]

The observed lasing threshold is over 3 orders of magnitude lower than for the previously reported optofluidic laser (440−530 μJ/mm^2) using aqueous microdroplet resonators that contained similar QD concentrations (1.3−2.6 μM).[34] Such significant improvement is due to the excellent Q-factor of the OFRR (~10^7).[38,39] The observed lasing threshold is also much lower than lasing threshold values reported in the OFRR laser demonstrations using organic dyes and green fluorescent proteins of similar concentrations (2−10 μM, 20−100 μJ/mm^2[14,39]), as the high absorption cross section at the pump wavelength of the QDs contributes to the significant reduction in the lasing threshold in the QD laser. Note that an extremely low lasing threshold (on the order of 1 μJ/mm^2) has also been achieved recently with densely packed thick QD films.[31] However, this demonstration required a QD density over 1000 times higher than in our case (interparticle distance: <10 nm vs ~100 nm in our case).

In order to understand the optofluidic QD laser, we write the threshold condition considering contributions due to multi-excitons within a QD.[48] We assume that filling of multiexciton states in a QD is governed by Poisson distribution. $P(N) = \langle N\rangle^N e^{-}\langle N\rangle/N!$ gives the probability of having N excitons in a given QD where $\langle N\rangle$ represents the average number of photogenerated excitons. For our relatively large, rod-like QDs, exciton−exciton interactions are much smaller than the emission bandwidth of around 80 meV. Assuming contributions from all multiexcitonic emission bands (single exciton, biexciton, triexciton, etc.), the lasing threshold condition can be written as

$$\sigma_{e,X}(\lambda_L)[n_T P(1)] + \sigma_{e,XX}(\lambda_L)[n_T P(2)] + \sigma_{e,XX}(\lambda_L)[n_T P(3)]... = \sigma_a(\lambda_L)[n_T P(0)] + \frac{\sigma_a(\lambda_L)}{2}[n_T P(1)] + \frac{2\pi m}{\lambda_L \eta Q_0} \quad (1)$$

where n_T is the total concentration of the QDs, $\sigma_{e,X}(\lambda_L)$ and $\sigma_{e,XX}(\lambda_L)$ are the single exciton and biexciton stimulated emission cross sections, $\sigma_a(\lambda_L)$ is the absorption cross section at the lasing wavelength (λ_L), η is the fraction of light in the evanescent field of the OFRR, Q_0 is the OFRR empty-cavity Q-factor, and m is the refractive index of the cavity mode ($m \approx 1.4$ for the OFRR).

The stimulated emission cross section of a laser transition can be related to the fluorescence lifetime (τ_F) by the following equation:[49]

$$\sigma_e(\lambda_L) = \frac{\lambda_L^4 E(\lambda_L)}{8\pi c n_L^2 \tau_F} \quad (2)$$

where $E(\lambda_L)$ is the fluorescence quantum distribution, n_L is the medium refractive index at λ_L, and c is the speed of light in a vacuum. For single exciton and biexciton emissions, the stimulated emission cross sections are determined by the radiative lifetimes of the transitions from the single exciton state ($|X\rangle$) to the ground state ($|0\rangle$) and two electron−hole pair state ($|XX\rangle$) to $|X\rangle$, respectively. Due to the 2-fold degeneracy of the 1S electron state, we can expect the radiative lifetime of the biexciton emission to be half of the radiative lifetime of single-exciton emission.[50] Based on eq 2, this implies the stimulated emission cross section for biexciton emission to be 2 times that of the single-exciton emission at a given emission wavelength, independent of the nonradiative Auger process decay rate. For this reason, in eq 1 the absorption of $|0\rangle$ is also considered to be 2 times larger than the absorption of $|X\rangle$. After substitutions of $\sigma_{e,XX}(\lambda_L) = 2\sigma_{e,X}(\lambda_L)$ and normalization condition of the Poisson distribution ($\sum_{i=0}^{\infty} P(i) = 1$), eq 1 can be written as

$$1 - P(0) - \frac{P(1)}{2} = \frac{\sigma_a(\lambda_L)}{\sigma_{e,XX}(\lambda_L)}P(0) + \frac{\sigma_a(\lambda_L)}{2\sigma_{e,XX}(\lambda_L)}P(1) + \frac{2\pi m}{\sigma_{e,XX}(\lambda_L) n_T \lambda_L \eta Q_0} \quad (3)$$

Using the experimentally measured data for the single-exciton transition, i.e., $n_L = 1.33$, $E(\lambda_L) = 0.0038$ nm^{-1} (see Supporting Information for detailed calculation), and $\tau_F = 33$ ns, we estimate $\sigma_{e,X}(\lambda_L)$ at $\lambda_L = 665$ nm to be $\sigma_{e,X}(\lambda_L) = 1.7 \times 10^{-17}$ cm^2 for our QDs, revealing the stimulated emission cross section for biexciton gain of $\sigma_{e,XX}(\lambda_L) = 3.4 \times 10^{-17}$ cm^2. This number is slightly smaller than the stimulated emission cross sections of good laser dyes ($\sigma_e(\lambda_L) \approx 1 \times 10^{-16}$ cm^2)[51] and conjugated polymers ($\sigma_e(\lambda_L) \approx 5 \times 10^{-17}$ cm^2)[52] and is comparable with the previous number obtained for biexciton gain in nanocrystal QDs.[27] Using other experimental parameters ($m = 1.4$, $\sigma_a(665\text{nm}) = 4.3 \times 10^{-16}$ cm^2, $n_T = 1.2 \times 10^{15}$ cm^{-3}, and $\eta Q_0 = 1 \times 10^7$[39,53]), eq 3 becomes

$$0.6758 = (13.6471 + 6.8235\langle N\rangle) \times e^{-\langle N\rangle} \quad (4)$$

revealing the number of average excitons per QD as $\langle N\rangle = 4.1$. Considering the QD absorption cross section at the pump wavelength (σ_a(433 nm) = 347 × 10^{-16} cm^2), and neglecting cavity-enhanced absorption effects, $\langle N\rangle = 4.1$ corresponds to a theoretical threshold fluence of $\Phi_{th} = 0.54$ μJ/mm^2,[54] which is slightly larger than the experimentally observed threshold fluence of 0.1 μJ/mm^2. Hence, we conclude that the overall QD gain that we observed experimentally is larger than our predictions. We attribute the difference between the observed and predicted threshold pump intensities to the quasi-one-dimensional nature of the rod-like QDs that we studied. In such QDs, the absence of quantum confinement in one dimension leads to an overall better optical gain performance.[55−58] We should also note that all our derivations in this paper assume steady-state conditions, which usually result in a higher threshold estimation. Accuracy of our predictions can be further increased by direct numerical solution of the rate equations.

Based on eq 3, the minimum QD concentration necessary for lasing can also be calculated by setting $P(0) = P(1) = 0$, i.e.,

$$n_{T\text{-min}} = \frac{2\pi m}{\sigma_{e,XX}(\lambda_L)\lambda_L \eta Q_0} \quad (5)$$

representing a very high pumping regime where $\langle N\rangle \gg 1$. For parameter values assumed in our calculations, the minimum concentration for QD lasing is obtained as $n_{T\text{-min}} = 0.65$ μM. It is important to emphasize that despite the fact that very low

DOI: 10.1021/acsphotonics.5b00211
ACS Photonics 2015, 2, 707−713

threshold lasing can be achieved with relatively low Q-factor resonators,[31] lasing with low QD concentrations (~1 μM) can only be achieved with a high-Q-factor resonator such as the OFRR.

We note that compared to the laser dyes ($\sigma_a(\lambda_P) \approx (1-10) \times 10^{-16}$ cm^2 and $\sigma_a(\lambda_L) \approx 10^{-19}$ cm^2),[51] the absorption cross sections of our QDs at λ_P and λ_L are at least ~2 orders of magnitude higher, which, together with the good stimulated emission cross section of our QDs and excellent Q-factors of the WGMs in the OFRR, is the main reason behind the observed ultralow threshold lasing. A large absorption cross section is an intrinsic property of the QDs related to their size, which is much larger than the size of an organic dye molecule.[19−21] In addition, our QDs have a rod-like geometry that further increases the absorption due to the behavior of their shell as an efficient antenna.[20,21]

Figure 3A and B show the photostability of lasing intensity obtained from 2 μM aqueous QDs kept still inside the OFRR

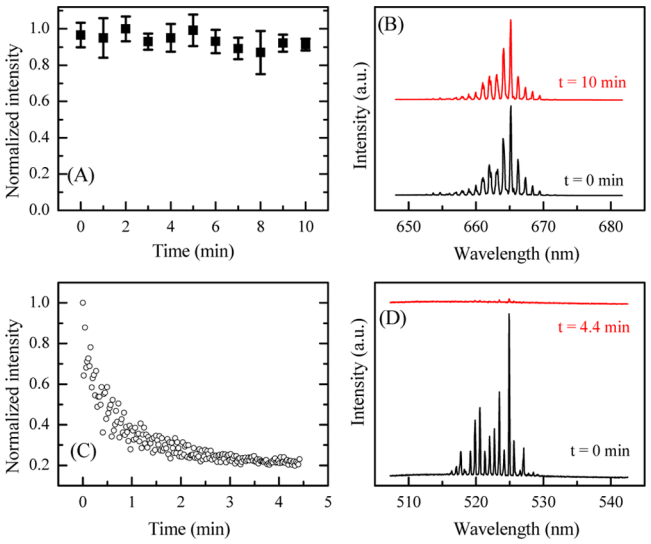

Figure 3. (A) Normalized lasing intensity integrated between 660 and 670 nm from 2 μM aqueous QDs over a duration of 10 min under 20 Hz pumping at an intensity of around 10× threshold (1.06 μJ/mm^2 per pulse). Error bars are obtained with three measurements. (B) QD lasing spectra recorded at t = 0 min and t = 10 min show negligible photobleaching. (C) Normalized lasing intensity integrated between 520 and 525 nm from 10 μM dye (fluorescein) over a duration of 4.4 min under 20 Hz pumping at an intensity of around 2.5× threshold (1.82 μJ/mm^2 per pulse). (D) Dye lasing spectra at t = 0 min and t = 4.4 min showing almost complete suppression of lasing due to dye photobleaching.

during 10 min (12 000 pulses in total) of uninterrupted pumping with a constant intensity of 1.06 μJ/mm^2 (~10× the lasing threshold). Spectra recorded during this time show no clear sign of photobleaching. The slight laser emission fluctuations can be mainly attributed to the fluctuations in the OPO output pulse energies. In contrast, photostability during such a long period of time cannot be achieved with a liquid dye laser when the liquid is kept still inside the laser cavity. Figure 3C and D show the results of our control experiments performed using a 10 μM fluorescein dye solution in water at an excitation wavelength of 493 nm and intensity of 1.82 μJ/mm^2 (2.5× the lasing threshold). Upon continuous pumping, the dye lasing intensity exhibits a relatively quick decrease (50% decrease within 30 s). Dye lasing is almost completely lost at around 4 min. Hence, the QD laser has significantly better photostability than the dye laser.

Not only have QDs been used for biosensing in bulk solution, they have also been used to perform biosensing where biological recognition (such as molecular binding) and detection take place at the interface between a solid substrate (such as glass) and aqueous solution. Therefore, in order to use QD lasers for surface-based biosensing in the future, it is critical to achieve QD lasing when they are immobilized on the surface. QD lasing from a very thick layer (0.5−1 μm) coated on a cylindrical ring resonator surface has previously been demonstrated.[29] However, this type of QD laser is not suitable for biosensing, as only the QDs on the topmost surface can be used for biosensing, and the remaining QDs underneath are not utilized, but simply contribute to the background.

Here, we employed surface immobilization biochemistry to attach a single layer of aqueous QDs on the inner surface of the OFRR (see the Supporting Information for details). After rinsing, the OFRR was subsequently filled with PBS buffer. Upon optical pumping, photostable QD lasing was observed as shown in Figure 4. As compared to the results presented in Figures 2 and 3 using aqueous QD solutions, the surface QD lasing threshold increases ~600-fold to 60 μJ/mm^2 and the center lasing wavelength blue-shifts by 10 nm to ~655 nm, very close to the QD fluorescence peak position. Both of these observations indicate a considerably smaller number of QDs coupled to the WGMs and are consistent with the dye laser behavior when the dye concentration is lowered.[39,59,60] However, despite the extremely high pumping intensity (199 μJ/mm^2, 3.5× higher than its threshold and ~200× larger than used in the bulk QD laser stability test in Figure 3), Figure 4B and C show that good photostability is still observed over the duration of 5 min (6000 pulses in total), more than enough for many biosensing applications. In comparison, dye and fluorescent proteins would be photobleached within only a few seconds under the same experimental conditions.[14] We further note that no indications of thermal degradation (*e.g.*, change in the emission band spectral profile) were observed in our lasing experiments with surface-immobilized QDs. We attribute this to the relatively low pump repetition rate used in our experiments.

For the case of surface-immobilized QD lasing, we calculate the stimulated emission cross section due to biexciton gain at the lasing wavelength (λ_L ~656 nm) to be $\sigma_e(\lambda_L) = 4.3 \times 10^{-17}$ cm^2. Due to the high threshold fluence observed in the case of lasing with QDs immobilized at the surface, eq 5 can be used to estimate the effective QD concentration as $n_{T\_eff} = 0.52$ μM. An upper limit for n_{T_eff} is given by the 2 μM concentration used in the bulk QD lasing case. Hence, we conclude that for the case of surface QD lasing 0.52 μM < n_{T_eff} < 2 μM. Considering the WGM decay length of 100 nm at a wavelength of 656 nm, we can estimate the QD surface density to be between 3.1×10^9 and 1.2×10^{10} cm^{-2},[14] which corresponds to 0.37−1.44% surface coverage considering QD dimensions of 8 × 15 nm or an average interparticle distance of 91−180 nm. We note that with this low surface density and the inherently small thickness of the immobilized QD layer determined by the size of a single QD, the profile of the lasing WGMs should not be significantly affected by the presence of the QDs at the inner surface of the OFRR.

By combining the excellent fluorescent properties of the state-of-the-art core/shell QDs with the unique properties of the OFRR as an optical cavity, we demonstrated optofluidic

DOI: 10.1021/acsphotonics.5b00211
ACS Photonics 2015, 2, 707−713

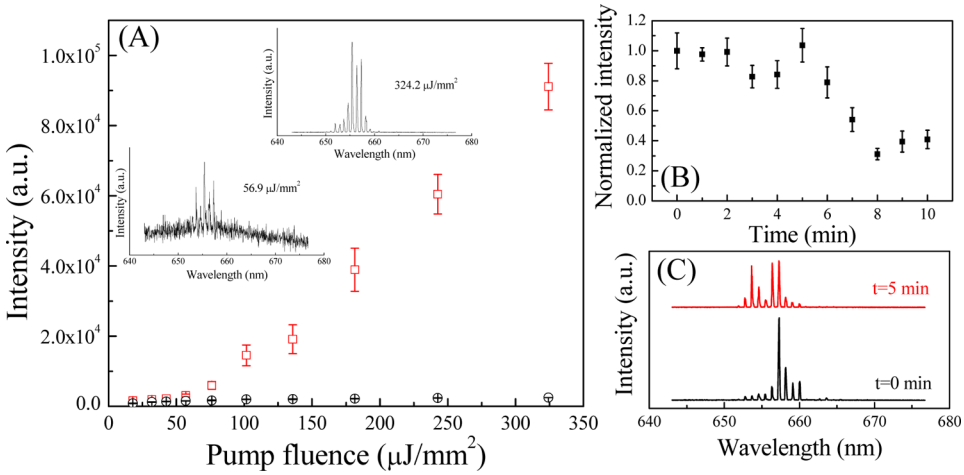

Figure 4. (A) Spectrally integrated intensity as a function of pump intensity for laser emission (squares) and fluorescence (circles) from a single layer of QDs immobilized on the inner surface of the ring resonator filled with PBS buffer solution. Spectral integration takes place in the range 653−658 nm for lasing and 644−649 nm for fluorescence, respectively. The lasing threshold is 60 μJ/mm^2 per pulse. Error bars are obtained with three measurements. Insets show examples of laser emission spectra at and well above the lasing threshold. (B) Normalized lasing intensity integrated between 650 and 660 nm over a duration of 10 min under a 20 Hz pumping at an intensity of 3.5× threshold (199 μJ/mm^2 per pulse) from a single layer of aqueous QDs immobilized on the inner surface of an OFRR. Error bars are obtained with three measurements. (C) QD lasing spectra recorded at t = 0 min and t = 5 min.

QD lasing using aqueous solutions. Our experiments employed aqueous QDs kept in solution inside the OFRR as well as those immobilized as a single layer on the inner surface of the OFRR. Thanks to the high absorption cross section of QDs and excellent Q-factor of the WGMs in the OFRR, lasing was achieved at ultralow pump intensities when a bulk QD solution was used as the laser gain medium. In both cases stable QD lasing was achieved for durations longer than 5 min, sufficient for many biosensing applications. Free from limitations posed by photobleaching, such optofluidic QD lasers are directly applicable to numerous applications in bioanalysis, where optofluidic dye lasers have already proven their superiority over spontaneous fluorescent emission-based measurements.

■ ASSOCIATED CONTENT

Supporting Information

Representative TEM image of the QDs, laser spot size analysis, absorption cross section measurement, quantum yield measurement, fluorescence lifetime measurement, fluorescence quantum distribution calculation, and procedure used for surface immobilization of QDs. The Supporting Information is available free of charge on the ACS Publications website at DOI: 10.1021/acsphotonics.5b00211.

■ AUTHOR INFORMATION

Corresponding Authors

*E-mail: (A. Kiraz) akiraz@ku.edu.tr.
*E-mail: (X. Fan) xsfan@umich.edu.

Author Contributions

A.K. and X.F. designed the research; A.K. and Q.C. performed the research; A.K., Q.C., and X.F. analyzed the data; and A.K., Q.C., and X.F. wrote the paper.

Notes

The authors declare no competing financial interest.

■ ACKNOWLEDGMENTS

A.K. acknowledges the support from a Fulbright Fellowship and the University of Michigan as a visiting scholar. Q.C. and X.F. acknowledge the support from the National Institutes of Health (1R21EB016783). We thank M. Tanyeri for fruitful discussions, M.-A. Mycek for QD lifetime measurement, and S. Sivaramakrishnan for absorption and quantum yield measurements.

■ REFERENCES

(1) Fan, X.; Yun, S.-H. The potential of optofluidic biolasers. *Nat. Methods* **2014**, *11*, 141−147.
(2) Fan, X.; White, I. M. Optofluidic microsystems for chemical and biological analysis. *Nat. Photonics* **2011**, *5*, 591−597.
(3) Schmidt, H.; Hawkins, A. R. The photonic integration of non-solid media using optofluidics. *Nat. Photonics* **2011**, *5*, 598−604.
(4) Zhang, X.; Lee, W.; Fan, X. Bio-switchable optofluidic lasers based on DNA Holliday junctions. *Lab Chip* **2012**, *12*, 3673−3675.
(5) Sun, Y.; Fan, X. Distinguishing DNA by analog-to-digital-like conversion by using optofluidic lasers. *Angew. Chem., Int. Ed.* **2012**, *51*, 1236−1239.
(6) Lee, W.; Fan, X. Intracavity DNA melting analysis with optofluidic lasers. *Anal. Chem.* **2012**, *84*, 9558−9563.
(7) Chen, Q.; Liu, H.; Lee, W.; Sun, Y.; Zhu, D.; Pei, H.; Fan, C.; Fan, X. Self-assembled DNA tetrahedral optofluidic lasers with precise and tunable gain control. *Lab Chip* **2013**, *13*, 3351−3354.
(8) Chen, Q.; Zhang, X.; Sun, Y.; Ritt, M.; Sivaramakrishnan, S.; Fan, X. Highly sensitive fluorescent protein FRET detection using optofluidic lasers. *Lab Chip* **2013**, *13*, 2679−2681.
(9) Jonáš, A.; Aas, M.; Karadag, Y.; Manioğlu, S.; Anand, S.; McGloin, D.; Bayraktarc, H.; Kiraz, A. In vitro and in vivo biolasing of fluorescent proteins suspended in liquid microdroplet cavities. *Lab Chip* **2014**, *14*, 3093−3100.
(10) Gather, M. C.; Yun, S. H. Single-cell biological lasers. *Nat. Photonics* **2011**, *5*, 406−410.
(11) Polson, R. C.; Vardeny, Z. V. Random lasing in human tissues. *Appl. Phys. Lett.* **2004**, *85*, 1289−1291.
(12) Song, Q.; Xiao, S.; Xu, Z.; Liu, J.; Sun, X.; Drachev, V.; Shalaev, V. M.; Akkus, O.; Kim, Y. L. Random lasing in bone tissue. *Opt. Lett.* **2010**, *35*, 1425−1227.
(13) Wu, X.; Khaing Oo, M. K.; Reddy, K.; Chen, Q.; Sun, Y.; Fan, X. Optofluidic laser for dual-mode sensitive biomolecular detection with a large dynamic range. *Nat. Commun.* **2014**, *5*, 3779.

DOI: 10.1021/acsphotonics.5b00211
ACS Photonics 2015, 2, 707−713

(14) Chen, Q.; Ritt, M.; Sivaramakrishnan, S.; Sun, Y.; Fan, X. Optofluidic lasers with a single molecular layer of gain. *Lab Chip* **2014**, *14*, 4590−4595.
(15) Pellegrino, T.; Manna, L.; Kudera, S.; Liedl, T.; Koktysh, D.; Rogach, A. L.; Keller, S.; Ra1dler, J.; Natile, G.; Parak, W. J. Hydrophobic nanocrystals coated with an amphiphilic polymer shell: A general route to water soluble nanocrystals. *Nano Lett.* **2004**, *4*, 703−707.
(16) Tomczak, N.; Jańczewski, D.; Han, M.; Vancso, G. J. Designer polymer-quantum dot architectures. *Prog. Polym. Sci.* **2009**, *34*, 393−430.
(17) Hu, X.; Gao, X. Silica-polymer dual layer-encapsulated quantum dots with remarkable stability. *ACS Nano* **2010**, *4*, 6080−6086.
(18) Wu, C.-S.; Khaing Ooa, M. K.; Cupps, J. M.; Fan, X. Robust silica-coated quantum dot−molecular beacon for highly sensitive DNA detection. *Biosens. Bioelectron.* **2011**, *26*, 3870−3875.
(19) Leatherdale, C. A.; Woo, W.-K.; Mikulec, F. V.; Bawendi, M. G. On the absorption cross section of CdSe nanocrystal quantum dots. *J. Phys. Chem. B* **2002**, *106*, 7619−7622.
(20) Talapin, D. V.; Koeppe, R.; Götzinger, S.; Kornowski, A.; Lupton, J. M.; Rogach, A. L.; Benson, O.; Feldmann, J.; Weller, H. Highly emissive colloidal CdSe/CdS heterostructures of mixed dimensionality. *Nano Lett.* **2003**, *3*, 1677−1681.
(21) Talapin, D. V.; Nelson, J. H.; Shevchenko, E. V.; Aloni, S.; Sadtler, B.; Alivisatos, A. P. Seeded growth of highly luminescent CdSe/CdS nanoheterostructures with rod and tetrapod morphologies. *Nano Lett.* **2007**, *7*, 2951−2959.
(22) Michalet, X.; Pinaud, F. F.; Bentolila, L. A.; Tsay, J. M.; Doose, S.; Li, J. J.; Sundaresan, G.; Wu, A. M.; Gambhir, S. S.; Weiss, S. Quantum dots for live cells, in vivo imaging, and diagnostics. *Science* **2005**, *307*, 538−544.
(23) Resch-Genger, U.; Grabolle, M.; Cavaliere-Jaricot, S.; Nitschke, R.; Nann, T. Quantum dots versus organic dyes as fluorescent labels. *Nat. Methods* **2008**, *5*, 763−775.
(24) Wu, C.-S.; Khaing Oo, M. K.; Fan, X. Highly sensitive multiplexed heavy metal detection using quantum-dot-labeled DNAzymes. *ACS Nano* **2010**, *4*, 5897−5904.
(25) Chen, Y.; Herrnsdorf, J.; Guilhabert, B.; Zhang, Y.; Watson, I. M.; Gu, E.; Laurand, N.; Dawson, M. D. Colloidal quantum dot random laser. *Opt. Express* **2011**, *19*, 2996−3003.
(26) Chan, Y.; Steckel, J. S.; Snee, P. T.; Caruge, J.-M.; Hodgkiss, J. M.; Nocera, D. G.; Bawendi, M. G. Blue semiconductor nanocrystal laser. *Appl. Phys. Lett.* **2005**, *86*, 073102.
(27) Klimov, V. I.; Mikhailovsky, A. A.; Xu, S.; Malko, A.; Hollingsworth, J. A.; Leatherdale, C. A.; Eisler, H.-J.; Bawendi, M. G. Optical gain and stimulated emission in nanocrystal quantum dots. *Science* **2000**, *290*, 314−317.
(28) Klimov, V. I.; Ivanov, S. A.; Nanda, J.; Achermann, M.; Bezel, I.; McGuire, J. A.; Piryatinski, A. Single-exciton optical gain in semiconductor nanocrystals. *Nature* **2007**, *447*, 441−446.
(29) Malko, A. V.; Mikhailovsky, A. A.; Petruska, M. A.; Hollingsworth, J. A.; Htoon, H.; Bawendi, M. G.; Klimov, V. I. From amplified spontaneous emission to microring lasing using nanocrystal quantumdot solids. *Appl. Phys. Lett.* **2002**, *81*, 1303−1305.
(30) Grivas, C.; Li, C.; Andreakou, P.; Wang, P.; Ding, M.; Brambilla, G.; Manna, L.; Lagoudakis, P. Single-mode tunable laser emission in the single-exciton regime from colloidal nanocrystals. *Nat. Commun.* **2013**, *4*, 2376.
(31) Dang, C.; Lee, J.; Breen, C.; Steckel, J. S.; Coe-Sullivan, S.; Nurmikko, A. Red, green and blue lasing enabled by single-exciton gain in colloidal quantum dot films. *Nat. Nanotechnol.* **2012**, *7*, 335−339.
(32) Menon, V. M.; Luberto, M.; Valappil, N. V.; Chatterjee, S. Lasing from InGaP quantum dots in a spin-coated flexible microcavity. *Opt. Express* **2008**, *16*, 19535−19540.
(33) Kazes, M.; Lewis, D. Y.; Ebenstein, Y.; Mokari, T.; Banin, U. Lasing from semiconductor quantum rods in a cylindrical microcavity. *Adv. Mater.* **2002**, *14*, 317−321.
(34) Schäfer, J.; Mondia, J. P.; Sharma, R.; Lu, Z. H.; Susha, A. S.; Rogach, A. L.; Wang, L. J. Quantum dot microdrop laser. *Nano Lett.* **2008**, *8*, 1709−1712.
(35) Wang, Y.; Leck, K. S.; Ta, V. D.; Chen, R.; Nalla, V.; Gao, Y.; He, T.; Demir, H. V.; Sun, H. Blue liquid lasers from solution of CdZnS/ZnS ternary alloy quantum dots with quasi-continuous pumping. *Adv. Mater.* **2015**, *27*, 169−175.
(36) White, I. M.; Oveys, H.; Fan, X. Liquid-core optical ring-resonator sensors. *Opt. Lett.* **2006**, *31*, 1319−1321.
(37) Han, K.; Kim, K. H.; Kim, J.; Lee, W.; Liu, J.; Fan, X.; Carmon, T.; Bahl, G. Fabrication and testing of microfluidic optomechanical oscillators. *J. Vis. Exp.* **2014**, *87*, e51497.
(38) Shopova, S. I.; Zhu, H.; Fan, X.; Zhang, P. Optofluidic ring resonator based dye laser. *Appl. Phys. Lett.* **2007**, *90*, 221101.
(39) Lacey, S.; White, I. M.; Sun, Y.; Shopova, S. I.; Cupps, J. M.; Zhang, P.; Fan, X. Versatile opto-fluidic ring resonator lasers with ultra-low threshold. *Opt. Express* **2007**, *15*, 17433−17442.
(40) Kim, K. H.; Bahl, G.; Lee, W.; Liu, J.; Tomes, M.; Fan, X.; Carmon, T. Cavity optomechanics on a microfluidic resonator with water and viscous liquids. *Light Sci. Appl.* **2013**, *2*, e110.
(41) White, I. M.; Gohring, J.; Sun, Y.; Yang, G.; Lacey, S.; Fan, X. Versatile waveguide-coupled opto-fluidic devices based on liquid core optical ring resonators. *Appl. Phys. Lett.* **2007**, *91*, 241104.
(42) Giepmans, B. N. G.; Deerinck, T. J.; Smarr, B. L.; Jones, Y. Z.; Ellisman, M. H. Correlated light and electron microscopic imaging of multiple endogenous proteins using quantum dots. *Nat. Methods* **2005**, *2*, 743−749.
(43) Louyer, Y.; Biadala, L.; Trebbia, J.-B.; Fernée, M. J.; Tamarat, P.; Lounis, B. Efficient biexciton emission in elongated CdSe/ZnS nanocrystals. *Nano Lett.* **2011**, *11*, 4370−4375.
(44) Xiao, J.; Wang, Y.; Hua, Z.; Wang, X.; Zhang, C.; Xiao, M. Carrier multiplication in semiconductor nanocrystals detected by energy transfer to organic dye molecules. *Nat. Commun.* **2012**, *3*, 1170.
(45) Lee, W.; Li, H.; Suter, J. D.; Reddy, K.; Sun, Y.; Fan, X. Tunable single mode lasing from an on-chip optofluidic ring resonator laser. *Appl. Phys. Lett.* **2011**, *98*, 061103.
(46) Lu, W.; Zhong, B.; Ma, D. Amplified spontaneous emission and gain from optically pumped films of dye-doped polymers. *Appl. Opt.* **2004**, *43*, 5074−5078.
(47) Ding, J.; Hagerott, M.; Ishihara, T.; Jeon, H.; Nurmikko, A. V. Zn,Cd)Se/ZnSe quantum-well lasers: Excitonic gain in an inhomogeneously broadened quasi-two-dimensional system. *Phys. Rev. B* **1993**, *47*, 10528−10542.
(48) Klimov, V. I. Spectral and dynamical properties of multiexcitons in semiconductor nanocrystals. *Annu. Rev. Phys. Chem.* **2007**, *58*, 635−673.
(49) Deshpande, A. V.; Beidoun, A.; Penzkofer, A.; Wagenblast, G. Absorption and emission spectroscopic investigation of cyanovinyldiethylaniline dye vapors. *Chem. Phys.* **1990**, *142*, 123−131.
(50) Wimmer, M.; Nair, S. V.; Shumway, J. Biexciton recombination rates in self-assembled quantum dots. *Phys. Rev. B* **2006**, *73*, 165305.
(51) Li, Z.; Psaltis, D. Optofluidic dye lasers. *Microfluid. Nanofluid.* **2008**, *4*, 145−158.
(52) Lawrence, J. R.; Turnbull, G. A.; Samuel, I. D. W. Broadband optical amplifier based on a conjugated polymer. *Appl. Phys. Lett.* **2002**, *80*, 3036−3038.
(53) Li, H.; Fan, X. Characterization of sensing capability of optofluidic ring resonator biosensors. *Appl. Phys. Lett.* **2010**, *97*, 011105.
(54) Mikhailovsky, A. A.; Malko, A. V.; Hollingsworth, J. A.; Bawendi, M. G.; Klimov, V. I. Multiparticle interactions and stimulated emission in chemically synthesized quantum dots. *Appl. Phys. Lett.* **2002**, *80*, 2380−2382.
(55) Cretí, A.; Zavelani-Rossi, M.; Lanzani, G.; Anni, M.; Manna, L.; Lomascolo, M. Role of the shell thickness in stimulated emission and photoinduced absorption in CdSe core/shell nanorods. *Phys. Rev. B* **2006**, *73*, 165410.
(56) Htoon, H.; Hollingworth, J. A.; Malko, A. V.; Dickerson, R.; Klimov, V. I. Light amplification in semiconductor nanocrystals:

DOI: 10.1021/acsphotonics.5b00211
ACS Photonics 2015, 2, 707−713

Quantum rods versus quantum dots. *Appl. Phys. Lett.* **2003**, *82*, 4776−4778.
(57) Htoon, H.; Hollingsworth, J.; Dickerson, R.; Klimov, V. Effect of zero- to one-dimensional transformation on multiparticle Auger recombination in semiconductor quantum rods. *Phys. Rev. Lett.* **2003**, *91*, 227401.
(58) Zavelani-Rossi, M.; Lupo, M. G.; Krahne, R.; Manna, L.; Lanzani, G. Lasing in self-assembled microcavities of CdSe/CdS core/shell colloidal quantum rods. *Nanoscale* **2010**, *2*, 931−935.
(59) Aas, M.; Jonáš, A.; Kiraz, A. Lasing in optically manipulated, dye-doped emulsion microdroplets. *Opt. Commun.* **2013**, *290*, 183−187.
(60) Tang, S. K. Y.; Li, Z.; Abate, A. R.; Agresti, J. J.; Weitz, D. A.; Psaltis, D.; Whitesides, G. M. A multi-color fast-switching microfluidic droplet dye laser. *Lab Chip* **2009**, *9*, 2767−2771.

DOI: 10.1021/acsphotonics.5b00211
ACS Photonics 2015, 2, 707−713